Molecular Cancer Therapeutics

TRX-E-002-1 Induces c-Jun–Dependent Apoptosis in Ovarian Cancer Stem Cells and Prevents Recurrence *In Vivo*

Ayesha B. Alvero[1], Andrew Heaton[2,3], Eydis Lima[1], Mary Pitruzzello[1], Natalia Sumi[1], Yang Yang-Hartwich[1], Carlos Cardenas[1], Sahra Steinmacher[1], Dan-Arin Silasi[1], David Brown[2,3], and Gil Mor[1,2]

Abstract

Chemoresistance is a major hurdle in the management of patients with epithelial ovarian cancer and is responsible for its high mortality. Studies have shown that chemoresistance is due to the presence of a subgroup of cancer cells with stemness properties and a high capacity for tumor repair. We have developed a library of super-benzopyran analogues to generate potent compounds that can induce cell death in chemoresistant cancer stem cells. TRX-E-002-1 is identified as the most potent analogue and can induce cell death in all chemoresistant $CD44^+/MyD88^+$ ovarian cancer stem cells tested ($IC_{50} = 50$ nmol/L). TRX-E-002-1 is also potent against spheroid cultures formed from cancer stem cells, chemosensitive $CD44^-/MyD88^-$ ovarian cancer cells, and heterogeneous cultures of ovarian cancer cells. Cell death was associated with the phosphorylation and increased levels of c-Jun and induction of caspases. *In vivo*, TRX-E-002-1 given as daily intraperitoneal monotherapy at 100 mg/kg significantly decreased intraperitoneal tumor burden compared with vehicle control. When given in combination with cisplatin, animals receiving the combination of cisplatin and TRX-E-002-1 showed decreased tumor burden compared with each monotherapy. Finally, TRX-E-002-1 given as maintenance treatment after paclitaxel significantly delayed disease recurrence. Our results suggest that TRX-E-002-1 may fill the current need for better therapeutic options in the control and management of recurrent ovarian cancer and may help improve patient survival. *Mol Cancer Ther; 15(6); 1279–90. ©2016 AACR.*

Introduction

Epithelial ovarian cancer is the most lethal of all gynecologic malignancies and the fourth leading cause of overall cancer deaths in women (1) with a dismal 5-year survival rate of 45.9% (2). Current standard of care consists of surgical debulking and adjuvant chemotherapy with platinum and taxane to which more than 80% of patients respond. Unfortunately, the majority of these patients eventually exhibit relapse (3), and upon disease recurrence, the value of the standard of care is limited by the presentation of carcinomatosis and chemoresistance. As such, the majority of patients with recurrent ovarian cancer eventually succumb to the disease.

Minimal advancement in the treatment of recurrent ovarian cancer has been made in the past decade. Most recent studies have highlighted the heterogeneity of ovarian tumors, and the current understanding is that inherently chemoresistant cancer stem cells that are not removed by surgery and survive first-line chemotherapy are able to recreate the tumor and cause disease recurrence (4–8). Our group and others have demonstrated that within the heterogeneous tumor, $CD44^+$ ovarian cancer cells represent the chemoresistant phenotype and, particularly, that the $CD44^+/MyD88^+$ ovarian cancer stem cell (OCSC) population represents the cancer cell type that can repair and rebuild the tumor (9–13). This cell population, therefore, represents the therapeutically relevant subtype that should be specifically targeted to prevent recurrence and improve patient survival. Our group has successfully used this system to establish screening models for the identification of better therapeutic options for ovarian cancer (14–17).

Flavonoids are a group of polyphenolic compounds found in plants that are characterized by a benzo-y-pyrone structure (18) and known to possess antitumor properties by inducing mitotic arrest and apoptosis (19). We have identified the core molecular structure required for benzopyran compounds to exert these functions and using this pharmacophore, we have created first- and second-generation drugs that exhibit significant activity against several types of cancer, including ovarian, both *in vitro* and *in vivo*. Phenoxodiol and triphendiol are first-generation compounds that have been shown to induce caspase-mediated cell death (20–25). In ovarian cancer, phenoxodiol acts as a chemosensitizer and thus lowers the IC_{50} for standard-of-care chemotherapy agents (20–22, 26, 27). NV-128 is a second-generation super-benzopyran (SBP) compound with a slightly more complex structure and more potent antitumor property, including activity against chemoresistant OCSC. Interestingly, NV-128 had a unique mechanism of action, such that in contrast

[1]Department of Obstetrics, Gynecology, and Reproductive Sciences, Yale University School of Medicine, New Haven, Connecticut. [2]CanTx, New Haven, Connecticut. [3]Novogen Ltd., Hornsby, New South Wales, Australia.

Note: Supplementary data for this article are available at Molecular Cancer Therapeutics Online (http://mct.aacrjournals.org/).

Corresponding Author: Gil Mor, Department of Obstetrics, Gynecology, and Reproductive Sciences, Yale University School of Medicine, Reproductive Immunology Unit, 333 Cedar Street, FMB 301, New Haven, CT 06520. Phone: 203-785-6294; Fax: 203-785-4883; E-mail: gil.mor@yale.edu

doi: 10.1158/1535-7163.MCT-16-0005

to phenoxodiol, which induced apoptosis, NV-128 induced caspase-independent cell death by targeting mitochondrial bioenergetics (14, 28).

To generate antitumor compounds with improved potency, we developed third-generation SBP analogues and screened them against chemoresistant OCSCs. In this study, we report the full preclinical work for TRX-E-002-1. We demonstrate the potency of this compound *in vitro* against chemoresistant OCSCs, and *in vivo* against an ovarian cancer mouse model, both at primary disease, and given as maintenance treatment. Furthermore, TRX-E-002-1 induces cell death by the activation and enhanced expression of c-Jun, leading to the induction of caspases.

Materials and Methods

Cell cultures and conditions

$CD44^+/MyD88^+$ OCSC clones (OCSC1 and OCSC2) and $CD44^-/MyD88^-$ ovarian cancer cells (OCC1 and OCC2) were isolated from either tumor tissue or ascites. These patient samples were obtained from patients at Yale New Haven Hospital (New Haven, CT) who were diagnosed with stage III/IV serous ovarian cancer and propagated as described previously (9, 10, 14, 28–33). Sample collection was performed with patient consent and approved by the Human Investigation Committee of Yale University School of Medicine (New Haven, CT). The epithelial nature of the isolated cells was determined by immunostaining for Ck18. Purity of the cultures based on CD44 expression by flow cytometry, MyD88 expression by Western blot analysis, and chemoresistance was determined by cell growth assays. The cells were isolated in early 2000, and these makers are routinely validated prior to each experiment. Stable expression of nuclear-restricted red fluorescent proteins (RFP; in OCSCs) or GFPs (in ovarian cancer cells) was performed by transduction using NucLight Red or Green Lentivirus Reagent (Essen BioScience). Spheroids were formed from OCSCs by culturing in Ultra-Low Attachment Multiwell Plates (Corning, Inc.).

Reagents and treatments

The SBP panel was obtained from Novogen Ltd. The synthesis of the SBP library was completed using a 4-step process comprised of acylation of a phenolic compound with a benzoic acid under phosphorous oxychloride/zinc chloride conditions; a cyclization using a substituted acetic acid; and Heunig's base, a global deprotection and partial reduction using a borane reagent and final catalytic reduction using palladium-based catalyst. The racemate was separated into two enantiomers using chiral SFC conditions with a Chiralcel OD-H column and carbon dioxide and methanol as mobile phases. Detailed synthetic information can be found in the WIPO patent no. WO2015117202. SP600125 and U0126 were obtained from Tocris (Bio-Techne). Cisplatin and paclitaxel used for *in vitro* testing were obtained from Sigma-Aldrich, Corp. For *in vivo* studies, cisplatin and paclitaxel were obtained from Mylan Institutional and APP Pharmaceuticals, respectively.

Real-time measurement of cell number and cell death and calculation of IC_{50}

Effect of each compound on cell morphology, growth, and viability was assessed using a kinetic Live-Cell Imaging System (IncuCyte, Essen BioScience). Proliferation was calculated as described previously (28, 34, 35) using metrics from either confluence or fluorescent count from nuclear-restricted RFP or GFP. Cell death was quantified similarly using CellTox Green Cytotoxicity Assay (Promega). IC_{50} was calculated as described previously (34) using GraphPad Prism (GraphPad Software Inc).

Caspase activity

Total protein was extracted and measured as described previously (19). Activity of caspase-3/7 and caspase-9 was quantified using Caspase-Glo Assay (Promega).

Western blot analysis

SDS-PAGE and Western blot analysis were performed using 20 μg of total protein lysate as described previously (19). Antibodies used were mouse anti-phospho ERK (Santa Cruz Biotechnology, Inc); rabbit anti-phospho c-Jun, rabbit anti c-Jun, rabbit anti-ERK, and rabbit anticleaved caspase-3, all from Cell Signaling Technology; and mouse anti-GAPDH (Sigma-Aldrich).

Mouse xenograft studies

The Yale University Institutional Animal Care and Use Committee approved all *in vivo* studies described. Intraperitoneal tumors were established in athymic nude mice using 4×10^6 $mCherry^+$ OCSC1-F2 ovarian cancer cells as described previously (35). Injection of cancer cells is designated as day 0, and treatment commenced between days 3 to 5. Establishment of intraperitoneal tumors was confirmed by live imaging (In-Vivo FX PRO, Bruker Corp) prior to treatment (36). TRX-E-002-1 was prepared in 20% sulfobutyl ether beta-cyclodextrin and administered daily at 50 or 100 mg/kg. Paclitaxel was given at 12 mg/kg every three days and cisplatin at 5 mg/kg weekly. All treatments were given intraperitoneally. Tumor growth was monitored every three days by live imaging, and response to treatment was assessed using (region of interest) ROI area as described previously (36, 37). Animals were sacrificed when tumor burden reached ROI = 120,000.

Statistical analysis

Data were graphed and analyzed using GraphPad Prism. Significance was calculated using two-way ANOVA with Dunnett correction for multiple comparisons, and $P < 0.05$ was considered significant.

Results

Identification of TRX-E-002 as a potent inducer of OCSC death

Our first objective was to identify potent SBP analogues from a panel of four different SBP subfamilies with cytotoxic activity against chemoresistant OCSCs. The analogues were screened against two clones of chemoresistant OCSCs (OCSC1 and OCSC2), which have demonstrated resistance to a variety of chemotherapeutic agents and thus represent the therapeutically relevant ovarian cancer cell subtype (9, 38–40). The efficacy of each analogue was based on its IC_{50}. Once an analogue demonstrated efficacy in the micromolar range, structural modifications were made using an iterative structure activity screening methodology, with the goal of increasing potency and achieving an IC_{50} in the nanomolar range. Of 40 analogues screened, we identified TRX-E-002, which was cytotoxic against the two clones of chemoresistant OCSCs with IC_{50} values < 0.245 μmol/L (Fig. 1A).

In vitro, conventional chemotherapeutic agents had negligible effect on OCSC growth even in the micromolar range (Supplementary Fig. S1). In contrast, TRX-E-002 showed a

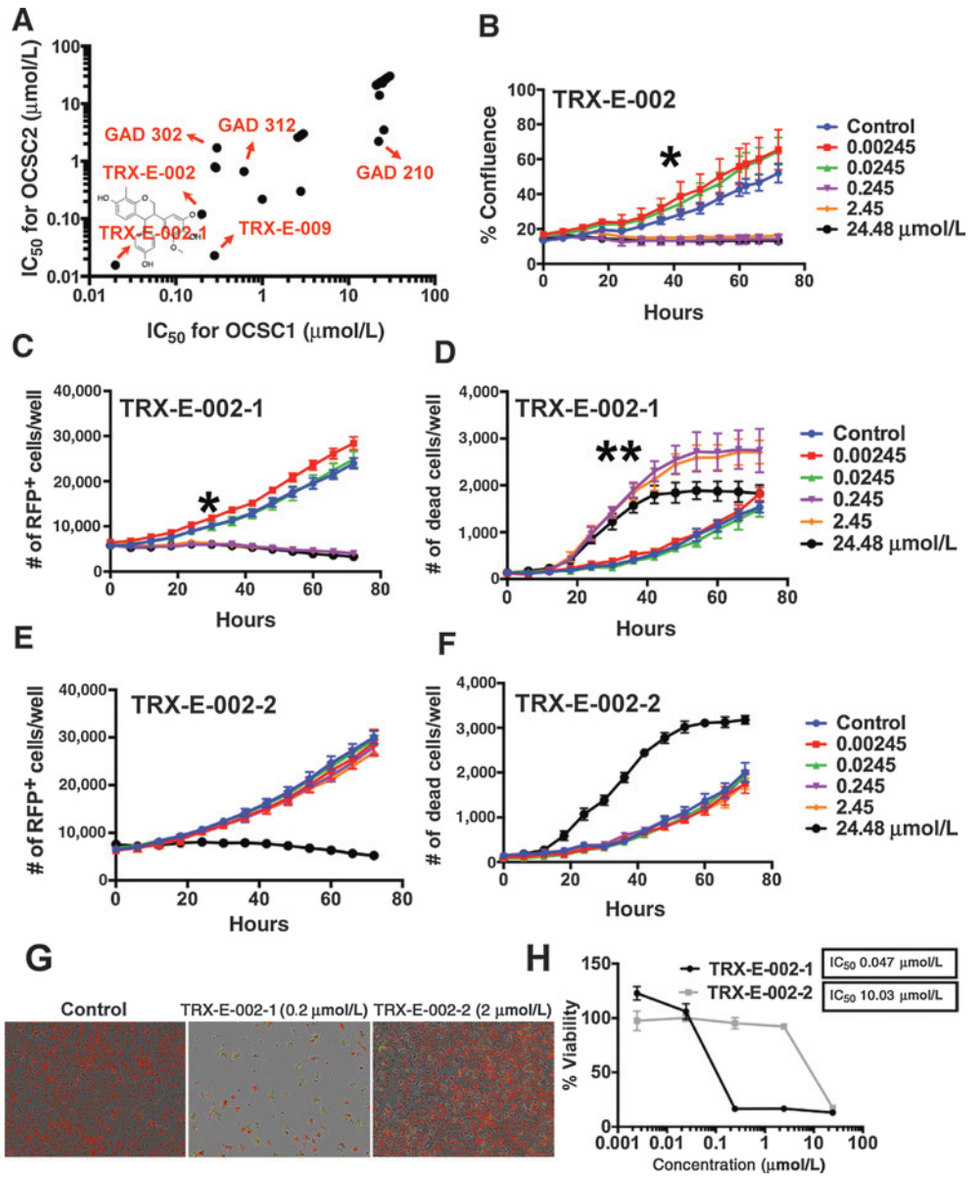

Figure 1.

TRX-E-002-1 demonstrates the best potency against chemoresistant OCSCs and performed better than standard of care. A, a panel of SBP analogues from three subfamilies was screened against two clones of chemoresistant $CD44^+/MyD88^+$ OCSCs. IC_{50} values for both clones are plotted. B, cell growth of OCSCs exposed to increasing concentrations of TRX-E-002; note the significant decrease in cell growth at doses 0.245 μmol/L and higher starting at the 48-hour time point, *, $P = 0.0097$, 0.0245, 0.007 comparing control with 0.245, 2.45, or 24.48 μmol/L doses, respectively; lower doses did not demonstrate statistical significance. C–F, TRX-E-002 enantiomers (TRX-E-002-1 and TRX-E-002-2) were separated and assessed separately in OCSCs by quantification of the number of RFP^+ cells and number of dead/CellTox-positive cells; note the significant decrease in the number of RFP^+ cells and significant increase in the number of dead cells at TRX-E-002-1 doses 0.245 μmol/L and higher starting at the 30-hour time point, *, $P = 0.0003$, 0.0009, 0.0004 comparing control with 0.245, 2.45, or 24.48 μmol/L, respectively; **, $P < 0.0003$, comparing control with doses 0.245 μmol/L and higher; lower doses did not demonstrate statistical significance. G and H, morphologic analysis and calculation of IC_{50} values demonstrate that TRX-E-002-1 is the active enantiomer; data shown are for OCSC2. Comparable results were obtained with OCSC1 and OCSC6.

persistent growth-inhibitory effect at these low concentrations (Fig 1B). Microscopic evaluation of the cultures showed a higher percentage of apoptotic cells in the TRX-E-002–treated cultures compared with those treated with cisplatin or paclitaxel (Supplementary Fig. S1). These results demonstrate that TRX-E-002 induces a rapid, persistent, and significant antitumor activity at low concentrations.

TRX-E-002-1 (enantiomer 1) is the active component of TRX-E-002

TRX-E-002 exists as a racemic mixture comprised of two enantiomers, enantiomer A (TRX-E-002-1) and enantiomer B (TRX-E-002-2). Thus, the enantiomers were separated and assessed separately. To distinguish between the cytostatic or cytotoxic activity of an analogue, we used OCSC clones that are stably transfected

with nuclear-restricted RFP, which allows an accurate quantification of the number of cells and can be multiplexed with CellTox Assay to concomitantly measure the number of dead and viable cells. We observed evidence of selective enantiomeric activity for enantiomer 1 or TRX-E-002-1, which elicits a significant decrease in the number of nuclear RFP^+ cells (Fig. 1C and Supplementary Movie S1A and S1B) and a concomitant increase in the number of CellTox-positive cells (Fig. 1D) beginning at the 0.245 μmol/L dose. In contrast, TRX-E-002-2 was mostly ineffective except for the very high dose of 10 μmol/L (Fig. 1E and F). Figure 1G shows the morphologic changes associated with the effect of these compounds on OCSC2. The IC_{50} for TRX-E-002-1 was 47 nmol/L, whereas the IC_{50} for TRX-E-002-2 was 10.03 μmol/L (Fig. 1H). On the basis of these results, TRX-E-002-1 was used as the active pharmaceutical ingredient to further characterize the cytotoxic effect on ovarian cancer cells.

Activity of TRX-E-002-1 against heterogeneous ovarian cancer cells

Once we established the efficacy of TRX-E-002-1 against chemoresistant OCSC, we determined its activity against two clones of chemosensitive ovarian cancer cells (OCC1 and OCC2; ref. 28). Our results show that TRX-E-002-1 was effective against both clones and was able to decrease the percentage of viable cells in a dose-dependent manner, with IC_{50} = 68 nmol/L and 27 nmol/L for OCC1 and OCC2, respectively (Supplementary Fig. S2A).

It is possible that response to chemotherapy may be modified by cross-talk among different cancer cell types within the tumor. Thus, to mimic the heterogeneity of ovarian tumors, we used an *in vitro* coculture model consisting of RFP-labeled chemoresistant OCSC2 and GFP-labeled chemosensitive OCC2. The cocultures, which were comprised of 50% RFP-OCSC2 and 50% GFP-OCC2 at the time of the treatment, were exposed to TRX-E-002-1, cisplatin, or the combination of both. As GFP-OCC2 has faster doubling time than RFP-OCSC2 (9), it overtook the control cocultures by the end of the experiment and thus the control cocultures are mainly comprised of GFP-OCC2 by the 24-hour time point (Fig. 2A). Cisplatin mainly affected GFP-OCC2, as evidenced by a decrease in the number of GFP^+ cells (Fig. 2B, left) but had no effect on the number of RFP^+ cells (Fig. 2B, right), demonstrating a lack of efficacy against the chemoresistant OCSC. Conversely, TRX-E-002-1 markedly reduced the number of both GFP-OCC2 and RFP-OCSC2, indicating that TRX-E-002-1 is highly potent against both ovarian cancer cell subtypes. The addition of cisplatin to TRX-E-002-1 enhanced the overall cytotoxic effect. These results suggest that the combination TRX-E-002-1 and cisplatin could be more effective in targeting heterogeneous ovarian cancer tumors.

TRX-E-002-1 is effective in inducing death in 3D ovarian cancer spheroids

Spheroids represent a 3D *in vitro* tumor model of multiple cell layers that mimic tumors *in vivo*. In ovarian cancer, spheroid cultures not only mimic ovarian solid tumors, but also ovarian cancer cells found in malignant ascites. Spheroid cultures allow us to test the capacity of compounds to diffuse through multiple layers of cells and induce cell death. More importantly, it allows us to test the efficacy of treatment against the mesenchymal cancer subtype. We previously showed that spheroid formation is a function of OCSCs and that this correlates with the acquisition of a mesenchymal phenotype, augmented migratory capacity, and enhanced chemoresistance (32). Thus, we tested the ability of TRX-E-002-1 to induce cell death in 3D spheroid cultures of OCSC2 by monitoring spheroid integrity using kinetic imaging. Compared with control, TRX-E-002-1 is able to significantly decrease the amount of intact spheroids in a dose-dependent manner (Fig. 2C) and is able to induce the collapse of their structure (Supplementary Fig. S2B). This is even more evident when we use GFP^+ OCSC2 spheroids. Although the control spheroids maintained structural integrity through time (Fig. 2D; Supplementary Movie S2A), TRX-E-002-1 was able to penetrate the multicellular layers of the spheroids and induce cell death in a time-dependent manner (Fig. 2D; Supplementary Movie S2B).

TRX-E-002-1 prevents OCSC recurrence *in vitro*

One of the main characteristics of OCSCs is their ability to overcome the cytotoxic effect of chemotherapeutic drugs even after 24 hours of treatment *in vitro* (35). To determine whether the cytotoxic effect of TRX-E-002-1 is sustained even after its removal, we treated OCSC2 with equivalent doses of TRX-E-002-1 or cisplatin for 24 hours and then removed the treatment allowing the culture to recover in growth media for another 48 hours. Our data show that in contrast to cisplatin, TRX-E-002-1 induced a persistent cytotoxic effect on OCSC2, and cells were not able to recover growth potential after 24 hours of treatment (Fig. 3A and B).

Next, we evaluated the minimum dose and time necessary for TRX-E-002-1 to confer a sustained cytotoxic effect. Thus, OCSC cells were exposed to different concentrations of TRX-E-002-1 for 2 hours and then allowed to recover in growth media for another 48 hours. We observed that 2 hours of exposure to 2.45 μmol/L of TRX-E-002-1 was sufficient to induce a sustained cytotoxic effect (Fig. 3C and D). However, when the concentration of TRX-E-002-1 was decreased to 0.245 μmol/L, 2 hours of exposure was not enough, and the cells were able to recover and resume proliferative potential (Fig. 3C and D). These results suggest that the molecular changes induced by TRX-E-002-1 during the 2-hour exposure with 2.45 μmol/L TRX-E-002-1 may be the key event responsible for its efficacy.

TRX-E-002-1–induced cell death is associated with phosphorylation and increased expression levels of c-Jun

To elucidate the early pathways responsible for the sustained cytotoxic effect observed with TRX-E-002-1, we performed a phosphokinase array that can detect relative phosphorylation levels of 43 different kinases involved in major signal transduction pathways. Compared with controls, cells treated with TRX-E-002-1 showed higher levels of phosphorylated c-Jun (p-c-Jun) and lower levels of phosphorylated-ERK (p-ERK; data not shown). These findings were validated by Western blot analysis, which showed a time-dependent increase in p-c-Jun accompanied by a time-dependent increase in total c-Jun (Fig. 4A). The Western blot analysis results also validated the decrease in p-ERK in cells treated with TRX-E-002-1. Interestingly, at baseline, the cells demonstrated cyclic ERK activation as evidenced by recurring upregulation and downregulation of p-ERK levels in no treatment controls through time. The effect on the phosphorylation status of the kinases (upregulation of p-c-Jun and downregulation of p-ERK) was observed as early as 2 hours posttreatment and maintained up to 24 hours (Fig. 4A). Interestingly, the phosphorylation levels of

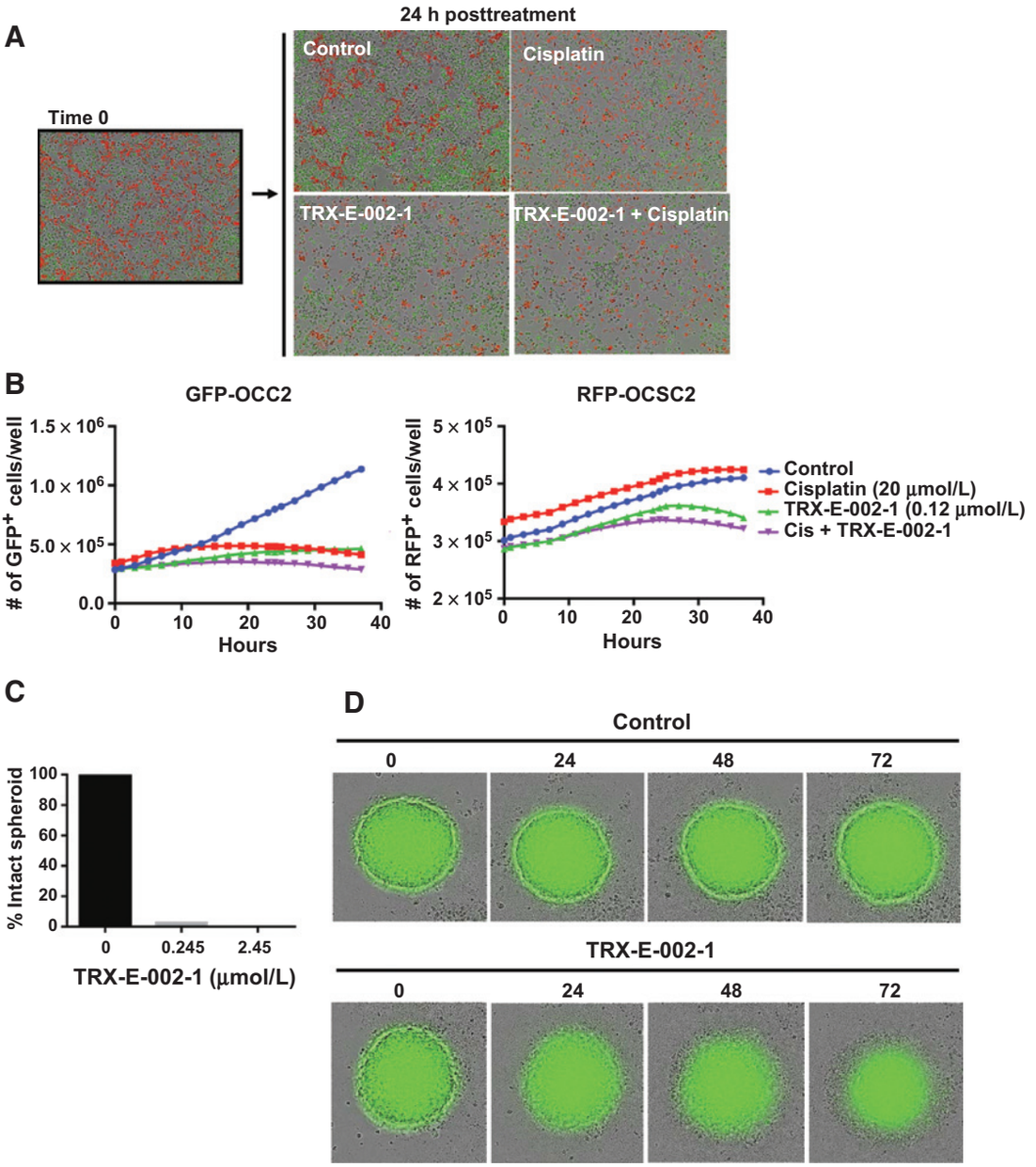

Figure 2.
TRX-E-002-1 is active against other relevant *in vitro* models of ovarian cancer cells. A, morphologic analysis of RFP$^+$ OCSC2 and GFP$^+$ OCC2 cocultured at 50/50 and treated with TRX-E-002-1 (0.12 μmol/L), cisplatin (Cis; 20 μmol/L), or the combination. B, quantification of cell number showing that TRX-E-002-1 is able to induce cell death on both cancer cell types. Data are presented as the effect of the treatments on each cell type differentiated by the fluorescent count. C, spheroids are formed from OCSCs, treated with TRX-E-002-1, and intact spheroids are quantified. D, composite images of control and TRX-E-002-1–treated GFP$^+$ OCSC spheroids through time; note the collapse of the outer ring on the TRX-E-002-1–treated spheroids.

c-Jun and ERK correlate with the differential ability of the two doses of TRX-E-002-1 to induce a sustained cytotoxic effect. As shown in Fig. 3B, treatment with 2.45 μmol/L TRX-E-002-1 for only 2 hours was enough to induce a sustained cytotoxic effect in OCSCs. This correlates with the ability of this dose of TRX-E-002-1 to maintain the upregulation of p-c-Jun and downregulation of p-ERK even when the compound is removed (Fig. 4B). In contrast, cells treated with of 0.245 μmol/L TRX-E-002-1 were able to recover proliferative potential (as shown in Fig. 3C) and were not able to sustain the increase in p-c-Jun and the decrease in p-ERK. As such, when the compound was removed after 2 hours, we observed that p-c-Jun and p-ERK returned to levels close to baseline (Fig. 4B). These data show that the sustained upregulation of p-c-Jun and downregulation of p-ERK are associated with TRX-E-002-1–induced cell death.

JNK is a stress-activated protein kinase and the main kinase that phosphorylates c-Jun (41–43). To determine whether the JNK/Jun pathway is required for TRX-E-002-1–induced cell

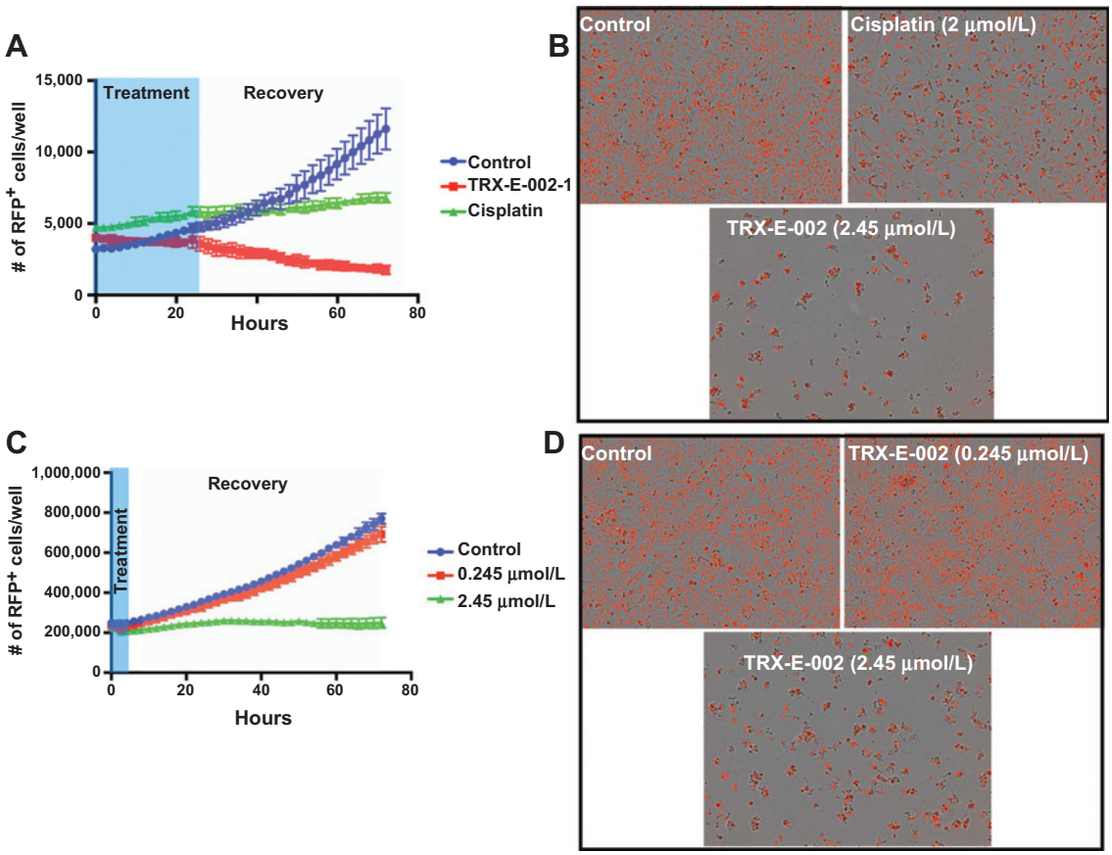

Figure 3.

TRX-E-002-1 treatment prevents *in vitro* recovery. A, OCSCs were treated with TRX-E-002-1 (2.45 μmol/L) or cisplatin (2 μmol/L) for 24 hours and allowed to recover in fresh growth media for another 48 hours. Note that in contrast to cisplatin, TRX-E-002-1 treatment prevented the recovery of OCSCs. B, composite images of OCSCs after 24-hour treatment and subsequent recovery. C, OCSCs were treated with increasing concentrations of TRX-E-002-1 for 2 hours and allowed to recover in fresh growth media for another 48 hours. Note that treatment with 2.45 μmol/L TRX-E-002-1 for only 2 hours is able to induce a sustained cytotoxic effect. D, composite images of OCSCs after 2-hour treatment and subsequent recovery.

death, we used the JNK inhibitor, SP600125, which is a reversible ATP competitive inhibitor selective for JNK 1, 2, and 3 (44). Thus cells were treated with TRX-E-002-1 in the presence or absence of SP600125. As shown in Fig. 4C, TRX-E-002-1 induced a significant increase in p-c-Jun, and this is abrogated with cotreatment with SP600125. In contrast, SP600125 did not affect the ability of TRX-E-002-1 to downregulate p-ERK, suggesting specificity of its activity against the c-Jun pathway (Fig. 4C). Determination of the effect on cell death showed that SP600125 cotreatment is able to rescue OCSCs from TRX-E-002-1–induced cell death (Fig. 4E). These results demonstrate the importance of c-Jun phosphorylation in TRX-E-002-1–induced cell death.

To determine the importance of downregulating the levels of p-ERK, cells were treated with U0126 to recapitulate the effect of TRX-E-002-1 on the ERK pathway. Western blot analysis showed that U0126 is able to downregulate the levels of p-ERK comparable with levels induced by TRX-E-002-1 (Fig. 4D). However, the effect of U0126 on cell death is not comparable with the effect of TRX-E-002-1 (Fig. 4F), suggesting that inhibition of the ERK pathway may not be relevant for the survival of OCSCs and, in addition, may not be required for TRX-002-1–induced cell death.

TRX-E-002-1 activates the apoptotic cascade

We then sought to determine whether the apoptotic pathway is involved in TRX-E-002-1–induced cell death. We assessed the activity of caspase-3/7 as well as caspase-9 at 2, 4, 6, 8, 16, and 24 hours posttreatment. TRX-E-002-1 was able to induce a significant increase in both caspase-3/7 (Fig. 5A) and caspase-9 (Fig. 5B) activity at 16 and 24 hours after treatment. These results demonstrate that TRX-E-002-1 is able to activate the apoptotic cascade in the chemoresistant OCSC cultures.

To determine the requirement for c-Jun activation in TRX-E-002-1–induced apoptosis, we used siRNA to knockdown c-Jun in chemoresistant OCSC. In cells transfected with scramble siRNA, we observed that, similar to results obtained with wild-type OCSC cells, TRX-E-002-1 is able to upregulate the levels of phospho-c-Jun and total c-Jun within two hours of treatment. This upregulation is maintained even when treatment was removed and cells were allowed to recover (Fig. 5C). The steady increase in the levels of phospho-c-Jun and total c-Jun in cells treated with TRX-E-002-1 correlates with the appearance of cleaved/active caspase-3. In contrast, in cells wherein c-Jun was knocked down, although TRX-E-002-1 is still able to upregulate the levels of phospho-c-Jun and total c-Jun compared with no treatment control, these

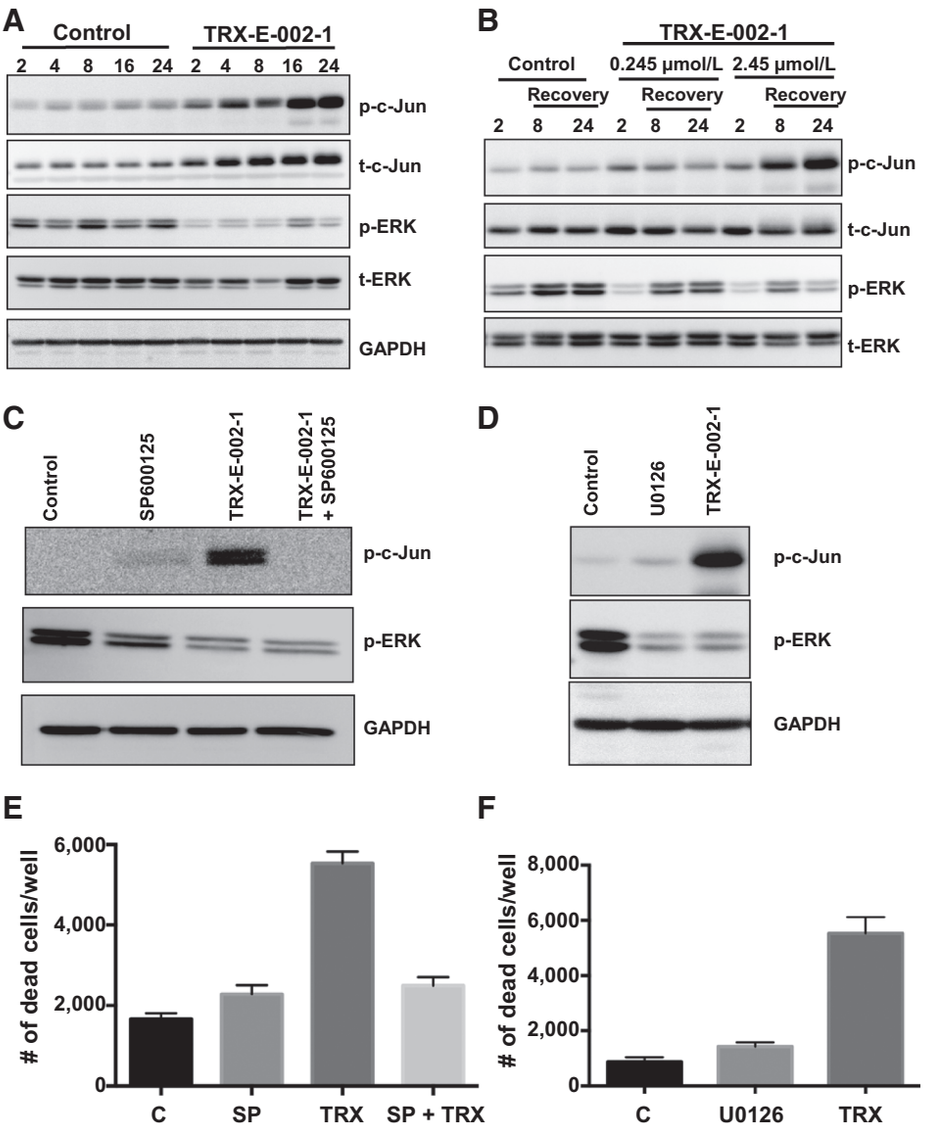

Figure 4.
c-Jun phosphorylation is associated with TRX-E-002-1–induced cell death. A, Western blot analysis for phosphorylated and total forms of c-Jun and ERK in OCSCs treated with 0.2 μmol/L TRX-E-002-1 at designated time points (in hours); B, OCSCs treated with either 0.2 or 2.45 μmol/L TRX-E-002-1 for 2 hours, followed by removal of the treatment and recovery in fresh growth media. Cells were collected at designated time points (in hours); note that sustained increase in p-c-Jun correlated with the inhibition of recovery shown in Fig. 3C. C, OCSCs were pretreated for 30 minutes with SP600125 (10 μmol/L) prior to adding TRX-E-002-1 (0.2 μmol/L). Samples were collected 2 hours after treatment and p-c-Jun and p-ERK levels determined by Western blot analysis. D, OCSCs were treated with the ERK inhibitor U0126 (10 μmol/L) or TRX-E-002-1 (0.2 μmol/L) for 2 hours. Samples were collected after treatment and p-c-Jun and p-ERK levels determined by Western blot analysis. E and F, parallel experiments as C and D were performed to determine the effect on cell death at 24-hour time point. C, control; SP, SP600125 (10 μmol/L), TRX, TRX-E-002-1 (0.2 μmol/L); U, U0126 (10 μmol/L).

levels are significantly less than observed in cells with scramble siRNA. Consequently, cleaved/active caspase-3 is not detectable.

In vivo activity of TRX-E-002-1 in an intraperitoneal ovarian cancer xenograft model

We previously described an intraperitoneal recurrent ovarian cancer xenograft model established using ovarian cancer cells stably expressing mCherry fluorescence. This allows the detection of intraperitoneal tumors and real-time measurement of response during the course of treatment (35–37). This model recapitulates the clinical profile typically seen in patients with ovarian cancer and allows us to answer three distinct questions: (i) *in vivo* activity of TRX-E-002-1 against primary disease; (ii) ability of TRX-E-002-1 given in combination with chemotherapy to prevent/delay recurrence; and (iii) ability of TRX-E-002-1 given as maintenance after chemotherapy to prevent/delay recurrence.

To determine the activity against primary disease as well as to determine the MTD, we performed a dose–response study. Mice receiving 150 mg/kg TRX-E-002-1 given i.p. three times weekly showed a significant decrease in tumor burden by the tenth dose, but response was accompanied by signs of toxicity (i.e., decreased mobility, weight loss, and neutropenia; Supplementary Fig. S3). In contrast, the lower doses of 50 and 100 mg/kg given daily i.p. maintained the compound's efficacy without the toxicity observed at the higher dose (Fig. 6A and Supplementary Fig. S4). Thus, mice receiving 50 mg/kg TRX-E-002-1 showed a significant reduction in tumor burden compared with vehicle control starting at day 14 ($P = 0.0004$), and mice receiving 100 mg/kg TRX-E-002-1 demonstrated significant reduction in tumor burden starting at day 10 compared with vehicle control ($P < 0.0001$). These significant reductions in tumor burden were maintained until the end of the treatment (Fig. 6A). Measurement of residual disease at the completion of the treatment showed a dose-dependent effect with mice

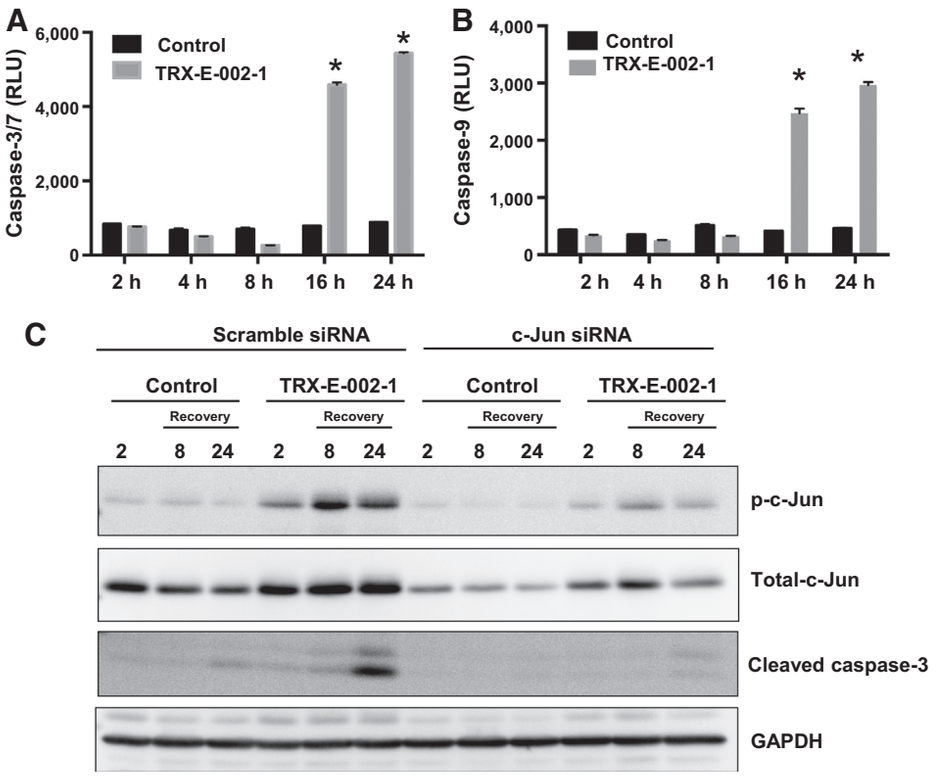

Figure 5.
TRX-E-002-1 activates the caspase cascade and requires c-Jun activation. A and B, OCSCs were treated with 0.245 μmol/L TRX-E-002-1; samples were collected at designated time points, and caspase-3 and caspase-9 activity was quantified by Caspase-Glo Assay. *, $P < 0.0001$ compared with no treatment control. C, OCSCs were transiently transfected with scramble siRNA or specific siRNA for c-Jun, treated with 2.45 μmol/L TRX-E-002-1 for 2 hours, and allowed to recover in growth media at designated time points (in hours). Note that TRX-E-002-1–induced increase in levels of total and p-c-Jun is lower in cells transfected with siRNA for c-Jun; this correlates with the absence of active caspase-3. RLU, relative luciferase units.

receiving daily 100 mg/kg TRX-E-002-1, demonstrating the best response and very little residual disease ($P < 0.0001$, compared with vehicle control; Fig. 6B and Supplementary Fig. S5A). Molecular analysis of these residual tumors showed the upregulation of both p-c-Jun and total c-Jun (Supplementary Fig. S5B). At this dose, we did not observe the neutropenia associated with the 150 mg/kg dose and observed only marginal weight loss (Supplementary Fig. S4). Although no animals required euthanasia due to morbidity, TRX-E-002-1 at 100 mg/kg daily was associated with abdominal distension, which was observed in 60% of animals at necropsy and primarily occurred in the cecal area. Animals were however able to recover from the distension upon cessation of treatment. These results demonstrate that TRX-E-002-1 given i.p. at 100 mg/kg daily was most efficacious and relatively well tolerated with no morbidity requiring euthanasia. Thus, we established the MTD at daily 100 mg/kg i.p., and this dose was employed for the succeeding studies employing combination treatment.

Addition of TRX-E-002-1 to cisplatin decreases tumor kinetics

Survival of chemoresistant OCSCs after chemotherapy has been attributed to disease recurrence and poor survival (9). We showed in our *in vitro* studies that the combination of TRX-E-002-1 and cisplatin was effective at targeting the heterogeneous cell culture comprised of chemosensitive and chemoresistant ovarian cancer cells. Thus, we next determined the value of adding TRX-E-002-1 to standard of care by comparing cisplatin monotherapy, TRX-E-002-1 monotherapy, or the combination. Animals received a total of 16 daily doses of TRX-E-002-1 (100 mg/kg) and 3 weekly doses of cisplatin (5 mg/kg), after which they were allowed to recover and continuously monitored. At day 47, 100% of the control animals and 80% to 83% of the animals receiving monotherapy reached the maximum allowed intraperitoneal tumor burden (as determined by ROI; Fig. 6C). In contrast, none of the animals in the combination group reached the maximum tumor burden (Fig. 6C). Thus, our results show that the combination of TRX-E-002-1 and cisplatin is able to decrease tumor kinetics better than monotherapy.

TRX-E-002-1 given as maintenance treatment after paclitaxel delays recurrence

Although the standard of care for ovarian cancer patients (platinum plus taxane) is effective initially, most patients develop recurrent disease (45). Recurrence is the major cause of mortality in ovarian cancer patients, and therefore, approaches that can prevent recurrence are critical to improve patient survival. As described previously, a unique advantage of our xenograft model is the recapitulation of recurrent disease that is typically observed in patients with ovarian cancer. As such, carcinomatosis is always observed and more importantly, although animals initially respond to paclitaxel, with some exhibiting complete response (i.e., no visible mCherry fluorescence detected by imaging), tumors eventually recur once paclitaxel treatment is terminated. Upon recurrence, tumors acquire resistance and become unresponsive to a second round of paclitaxel regimen (46), as observed in ovarian cancer patients. Therefore, the model allows us to assess the value of novel compounds in preventing recurrence when given as maintenance treatment. Thus, mice were given paclitaxel as initial treatment. Similar to our previous observation (35), this resulted in a significant delay in tumor progression (Fig. 6D and E). After the fourth dose of paclitaxel, mice were rerandomized into the different maintenance groups.

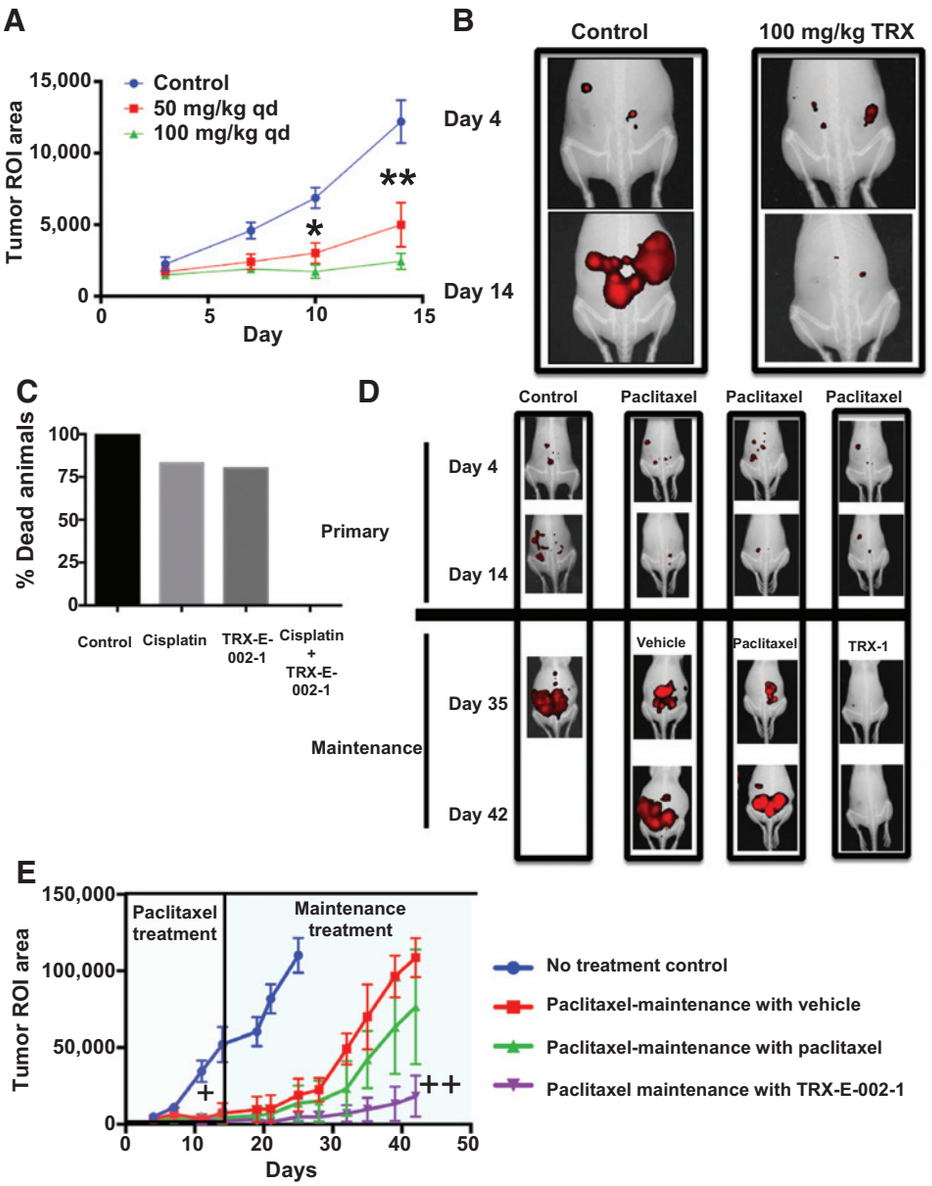

Figure 6.
TRX-E-002-1 demonstrates significant antitumor activity against both primary and recurrent disease in a mouse xenograft model of ovarian cancer. Treatment of primary disease: once tumors were detected by live imaging, mice were treated intraperitoneally with 50 or 100 mg/kg TRX-E-002-1 daily (qd). A, tumor growth curves as measured using mCherry fluorescence area; *, $P = 0.0029$ and $P < 0.0001$, control versus 50 or 100 mg/kg, respectively; **, $P < 0.0001$, control versus both doses. B, representative images showing response of mCherry$^+$ tumors. C, combination treatment with TRX-E-002-1 and cisplatin: mice were treated with cisplatin (3 doses at 5 mg/kg given weekly), TRX-E-002-1 (16 doses at 100 mg/kg given daily), or the combination of both. Percentage of dead animals at day 47 is shown. D, maintenance treatment: once tumors were established and detected by live imaging, mice were treated with paclitaxel (4 doses at 12 mg/kg) then rerandomized to designated maintenance treatments. Representative images showing mCherry$^+$ tumors. E, tumor growth curves during the first-line treatment with paclitaxel (gray box) and maintenance treatment (blue box); +, $P < 0.0001$, control versus first-line paclitaxel; ++, $P < 0.0001$, TRX-E-002-1 maintenance versus paclitaxel maintenance.

Here, the maintenance protocol consisted of continued treatment with paclitaxel, maintenance with TRX-E-002-1 (100 mg/kg), or maintenance with vehicle control. As is observed in patients who relapse with drug-resistant disease, tumor progression was observed in the group maintained with paclitaxel, indicating the tumors had acquired paclitaxel resistance. In contrast, daily intraperitoneal maintenance with TRX-E-002-1 was able to effectively retard tumor proliferation. Analysis of ROI area showed that by day 35, tumor burden in the TRX-E-002-1–maintained group was significantly less than the group maintained with paclitaxel ($P = 0.003$; Fig. 6E). Tumor weights at the endpoint were also significantly reduced in the TRX-E-002-1–maintained group compared with control ($P = 0.008$), but not in paclitaxel-maintained group when compared with control ($P = 0.2052$; Supplementary Fig. S5C). Gross examination of residual disease showed that mice maintained with paclitaxel and mice maintained with vehicle had visible carcinomatosis and extensive metastasis in the diaphragm, peritoneum, and adipose tissue. In contrast, in mice maintained with TRX-E-002-1, we observed microscopic metastasis mainly in the adipose tissue (data not shown). Animals appeared to tolerate this schedule of TRX-E-002-1 with no signs of disease or morbidity requiring euthanasia. Taken together, our results demonstrate the value of TRX-E-002-1 in the first-line setting as an addition to standard of care and also in the maintenance setting as an adjuvant treatment after the completion of first-line standard of care.

Discussion

We describe in this study the identification of TRX-E-002-1, a novel SBP molecule with significant potency against relevant *in vitro* and *in vivo* models of ovarian cancer. We identified TRX-E-002-1 by screening different structural modifications of the parental SBP scaffold against the chemoresistant OCSCs and further

validated its antitumor activity on different ovarian cancer cell subtypes and an orthotopic ovarian cancer xenograft model. We showed that it mainly affects c-Jun phosphorylation and enhanced expression, leading to caspase activation and cell death. The efficacy was demonstrated *in vivo* in a highly resistant ovarian cancer animal model in the treatment of primary disease, both as monotherapy and in combination with cisplatin. We also showed its value in maintenance therapy, wherein it is able to curtail tumor kinetics and consequently delay disease recurrence.

The survival rate in ovarian cancer has not improved since the introduction of combination chemotherapy several decades ago. Although effective in the treatment of primary disease, patients eventually recur and present with chemoresistance and carcinomatosis (45). Current studies suggest that recurrence is caused by the regrowth of the surviving inherently chemoresistant cancer stem cells that persisted during chemotherapy. The expansion of this chemoresistant cancer cell population, coupled with prosurvival modifications induced by the pressure of treatment, is thought to be responsible for the development of chemoresistant recurrent disease (10). Heterogeneity of ovarian tumors is not only limited to the presence of different epithelial cell subtypes with differential stemness potential, but also in the presence of different cancer cells with varying stages of mesenchymal status and migratory/invasiveness potential (9, 47). Therefore to improve survival, a practical approach is the use of novel therapies that can induce cell death in these various subtypes of ovarian cancer cells. Indeed, we demonstrate that TRX-E-002-1 is able to induce cell death in chemoresistant $CD44^+/MyD88^+$ OCSC clones, as well as in chemosensitive $CD44^-/MyD88^-$ ovarian cancer cell lines both when grown separately or in cocultures, which mimic tumor heterogeneity. Moreover, we show that TRX-E-002-1 is potent against ovarian cancer cell spheroids and can induce the fragmentation of these 3D cultures.

The ovarian cancer xenograft model used in this study recapitulates the clinical profile observed in patients, such as carcinomatosis and the initial responsiveness to chemotherapy with subsequent presentation of chemoresistant recurrent disease (35–37). As part of first-line treatment, we demonstrated the efficacy of TRX-E-002-1 given as a monotherapy, and as part of combination treatment. We also showed that it is not antagonistic to current standard of care and can improve outcomes in mice. As part of maintenance therapy, TRX-E-002-1 is able to delay recurrence when given after chemotherapy. By decreasing tumor growth kinetics in recurrent disease, TRX-E-002-1 treatment resulted in lower tumor burden, which can significantly improve surgical debulking. This is important as the capacity of surgeons to perform optimal debulking and minimize residual disease has been shown to directly correlate with survival and is the best prognostic factor in ovarian cancer (48).

Molecular analysis demonstrates the opposing effect of TRX-E-002-1 on the Jun pathway and the ERK pathway. Interestingly, despite the high levels of baseline ERK activation, the ovarian cancer cells tested do not depend on ERK signaling for survival. Thus, although TRX-E-002-1 can significantly downregulate the levels of p-ERK, simulating ERK inhibition using a MEK inhibitor did not lead to cell death. These results have clinical implications, especially in patients with low-grade serous ovarian cancer, wherein the Ras/Raf pathway is mutated (49). It is possible that these mutations, or any other epigenetic changes that can lead to elevated baseline levels of p-ERK, may not necessarily be significant drivers of the disease.

TRX-E-002-1–induced cell death instead is associated with the persistent activation and enhanced expression levels of c-Jun. c-Jun is involved in cellular processes as diverse as proliferation, differentiation, and death (50). In most cells, c-Jun is regulated by phosphorylation, which can be initiated by multiple stimuli. The eventual outcome from this wide range of inputs to c-Jun further depends on the cell type and current cellular state. It has been demonstrated that to activate cell death pathways, c-Jun activation and stabilization should be persistent instead of transient (51). Indeed, this is what we observed during TRX-E-002-1–induced cell death. Phosphorylation of c-Jun occurs as early as 2 hours and persisted up to 16 to 24 hours when significant caspase activation and cell death has occurred. This is accompanied by steady increase in the levels of total c-Jun, which may be due to a combination of transcription/translation of new protein and stabilization of already occurring c-Jun proteins (50, 52). The mechanism by which TRX-E-002-1 stabilizes c-Jun is currently under investigation.

It is important to emphasize that at specific doses, TRX-E-002-1 can persistently activate c-Jun even when cells are exposed for only a short period of time. In cells treated with 2.45 μmol/L of TRX-E-002-1 for 2 hours and allowed to recover in growth media, phosphorylation of c-Jun as well as total levels of c-Jun steadily increased. This highlights the importance of reaching the optimal dose and time of exposure *in vivo* and suggests the value of c-Jun as a biomarker for response. Indeed we show that c-Jun phosphorylation can be detected *in vivo*.

In conclusion, we describe a complete preclinical study justifying the use of TRX-E-002-1 in ovarian cancer. The compound may fill the current need for better therapeutic options in the control and management of recurrent ovarian cancer and may help improve patient survival. Results from in-human trials will conclusively show the value of TRX-E-002-1 in ovarian cancer and possibly other types of intra-abdominal cancers.

Disclosure of Potential Conflicts of Interest

A.B. Alvero has ownership interest (including patents) in TRX-E-002-1. D. Brown has ownership interest (including patents) in Novogen Ltd. G. Mor reports receiving a commercial research grant from CanTx. No potential conflicts of interest were disclosed by the other authors.

Authors' Contributions

Conception and design: A.B. Alvero, D. Brown, G. Mor

Development of methodology: A. Heaton, E. Lima, M. Pitruzzello, N. Sumi, G. Mor

Acquisition of data (provided animals, acquired and managed patients, provided facilities, etc.): E. Lima, N. Sumi, D.-A. Silasi

Analysis and interpretation of data (e.g., statistical analysis, biostatistics, computational analysis): A.B. Alvero, E. Lima, M. Pitruzzello, Y. Yang-Hartwich, G. Mor

Writing, review, and/or revision of the manuscript: A.B. Alvero, E. Lima, D.-A. Silasi, D. Brown, G. Mor

Administrative, technical, or material support (i.e., reporting or organizing data, constructing databases): E. Lima, M. Pitruzzello, C. Cardenas, S. Steinmacher

Other (company liaison): D. Brown

Acknowledgments

The authors thank JoAnn Bilyard for reviewing the manuscript.

Grant Support

This study was supported in part by a grant from CanTx and the Discovery to Cure Research Program (to G. Mor).

The costs of publication of this article were defrayed in part by the payment of page charges. This article must therefore be hereby marked *advertisement* in accordance with 18 U.S.C. Section 1734 solely to indicate this fact.

Received January 12, 2016; revised March 16, 2016; accepted March 28, 2016; published OnlineFirst April 8, 2016.

References

1. Siegel R, Ma J, Zou Z, Jemal A. Cancer statistics, 2014. CA Cancer J Clin 2014;64:9–29.
2. Howlader N, Noone AM, Krapcho M, Garshell J, Miller D, Altekruse SF, et al. SEER Cancer Statistics Review, 1975–2011. Bethesda, MD: NCI; 2014. Available from: http://seer.cancer.gov/csr/1975_2012/.
3. Katsumata N, Yasuda M, Isonishi S, Takahashi F, Michimae H, Kimura E, et al. Long-term results of dose-dense paclitaxel and carboplatin versus conventional paclitaxel and carboplatin for treatment of advanced epithelial ovarian, fallopian tube, or primary peritoneal cancer (JGOG 3016): a randomised, controlled, open-label trial. Lancet Oncol 2013;14:1020–6.
4. Clarke MF, Dick JE, Dirks PB, Eaves CJ, Jamieson CH, Jones DL, et al. Cancer stem cells–perspectives on current status and future directions: AACR Workshop on cancer stem cells. Cancer Res 2006;66:9339–44.
5. Dalerba P, Cho RW, Clarke MF. Cancer stem cells: models and concepts. Annu Rev Med 2007;58:267–84.
6. Hemmings C.The elaboration of a critical framework for understanding cancer: the cancer stem cell hypothesis. Pathology 2010;42: 105–12.
7. Morrison R, Schleicher SM, Sun Y, Niermann KJ, Kim S, Spratt DE, et al. Targeting the mechanisms of resistance to chemotherapy and radiotherapy with the cancer stem cell hypothesis. J Oncol 2011;2011:941876.
8. Winquist RJ, Furey BF, Boucher DM. Cancer stem cells as the relevant biomass for drug discovery. Curr Opin Pharmacol 2010;10:385–90.
9. Alvero AB, Chen R, Fu HH, Montagna M, Schwartz PE, Rutherford T, et al. Molecular phenotyping of human ovarian cancer stem cells unravels the mechanisms for repair and chemoresistance. Cell Cycle 2009;8:158–66.
10. Chefetz I, Alvero AB, Holmberg JC, Lebowitz N, Craveiro V, Yang-Hartwich Y, et al. TLR2 enhances ovarian cancer stem cell self-renewal and promotes tumor repair and recurrence. Cell Cycle 2013;12:511–21.
11. Meng E, Long B, Sullivan P, McClellan S, Finan MA, Reed E, et al. CD44+/CD24- ovarian cancer cells demonstrate cancer stem cell properties and correlate to survival. Clin Exp Metastasis 2012;29:939–48.
12. Rodriguez-Rodriguez L, Sancho-Torres I, Mesonero C, Gibbon DG, Shih WJ, Zotalis G. The CD44 receptor is a molecular predictor of survival in ovarian cancer. Med Oncol 2003;20:255–63.
13. Steg AD, Bevis KS, Katre AA, Ziebarth A, Dobbin ZC, Alvarez RD, et al. Stem cell pathways contribute to clinical chemoresistance in ovarian cancer. Clin Cancer Res 2012;18:869–81.
14. Alvero AB, Montagna MK, Chen R, Kim KH, Kyungjin K, Visintin I, et al. NV-128, a novel isoflavone derivative, induces caspase-independent cell death through the Akt/mammalian target of rapamycin pathway. Cancer 2009;115:3204–16.
15. Chefetz I, Holmberg JC, Alvero AB, Visintin I, Mor G. Inhibition of Aurora-A kinase induces cell cycle arrest in epithelial ovarian cancer stem cells by affecting NFkB pathway. Cell Cycle 2011;10:2206–14.
16. Green JM, Alvero AB, Kohen F, Mor G. 7-(O)-Carboxymethyl daidzein conjugated to N-t-Boc-hexylenediamine: a novel compound capable of inducing cell death in epithelial ovarian cancer stem cells. Cancer Biol Ther 2009;8:1747–53.
17. Kim KH, Xie Y, Tytler EM, Woessner R, Mor G, Alvero AB. KSP inhibitor ARRY-520 as a substitute for Paclitaxel in Type I ovarian cancer cells. J Transl Med 2009;7:63.
18. Yao LH, Jiang YM, Shi J, Tomas-Barberan FA, Datta N, Singanusong R, et al. Flavonoids in food and their health benefits. Plant Foods Hum Nutr 2004;59:113–22.
19. Kamsteeg M, Rutherford T, Sapi E, Hanczaruk B, Shahabi S, Flick M, et al. Phenoxodiol–an isoflavone analog–induces apoptosis in chemoresistant ovarian cancer cells. Oncogene 2003;22:2611–20.
20. Alvero AB, Rossi P, Brown D, Leizer A, Kelly M, Rutherford T, Husband A, Mor G. Phenoxodiol—A chemosensitizer in the midst of cancer chemoresistance. US Oncology 2008;4:39–41.
21. Alvero AB, Brown D, Montagna M, Matthews M, Mor G. Phenoxodiol-Topotecan co-administration exhibit significant anti-tumor activity without major adverse side effects. Cancer Biol Ther 2007;6:612–7.
22. Alvero AB, O'Malley D, Brown D, Kelly G, Garg M, Chen W, et al. Molecular mechanism of phenoxodiol-induced apoptosis in ovarian carcinoma cells. Cancer 2006;106:599–608.
23. Wang X, McKernan R, Kim KH, Alvero AB, Whiting A, Thompson JA, et al. Triphendiol (NV-196), development of a novel therapy for pancreatic cancer. Anticancer Drugs 2011;22:719–31.
24. Aguero MF, Facchinetti MM, Sheleg Z, Senderowicz AM. Phenoxodiol, a novel isoflavone, induces G1 arrest by specific loss in cyclin-dependent kinase 2 activity by p53-independent induction of p21WAF1/CIP1. Cancer Res 2005;65:3364–73.
25. Alvero AB, Kelly M, Rossi P, Leiser A, Brown D, Rutherford T, et al. Anti-tumor activity of phenoxodiol: from bench to clinic. Future Oncol 2008;4:475–82.
26. Rutherford T, O'malley D, Makkenchery A, Baker L, Azodi M, Schwartz P, et al. Phenoxodiol phase Ib/II study in patients with recurrent ovarian cancer that resistant to second line chemotherapy. J Soc Gynecol Investig 2004;11:254.
27. Sapi E, Alvero AB, Chen W, O'Malley D, Hao XY, Dwipoyono B, et al. Resistance of ovarian carcinoma cells to docetaxel is XIAP dependent and reversible by phenoxodiol. Oncol Res 2004;14:567–78.
28. Alvero AB, Montagna MK, Holmberg JC, Craveiro V, Brown D, Mor G. Targeting the mitochondria activates two independent cell death pathways in ovarian cancer stem cells. Mol Cancer Ther 2011;10: 1385–93.
29. Alvero AB, Fu HH, Holmberg J, Visintin I, Mor L, Marquina CC, et al. Stem-like ovarian cancer cells can serve as tumor vascular progenitors. Stem Cells 2009;27:2405–13.
30. Alvero AB, Montagna MK, Craveiro V, Liu L, Mor G. Distinct subpopulations of epithelial ovarian cancer cells can differentially induce macrophages and T regulatory cells toward a pro-tumor phenotype. Am J Reprod Immunol 2012;67:256–65.
31. Alvero AB, Montagna MK, Sumi NJ, Joo WD, Graham E, Mor G. Multiple blocks in the engagement of oxidative phosphorylation in putative ovarian cancer stem cells: implication for maintenance therapy with glycolysis inhibitors. Oncotarget 2014;5:8703–15.
32. Yin G, Alvero AB, Craveiro V, Holmberg JC, Fu HH, Montagna MK, et al. Constitutive proteasomal degradation of TWIST-1 in epithelial-ovarian cancer stem cells impacts differentiation and metastatic potential. Oncogene 2013;32:39–49.
33. Yin G, Chen R, Alvero AB, Fu HH, Holmberg J, Glackin C, et al. TWISTing stemness, inflammation and proliferation of epithelial ovarian cancer cells through MIR199A2/214. Oncogene 2010;29:3545–53.
34. Artymovich K, Appledorn DM. A multiplexed method for kinetic measurements of apoptosis and proliferation using live-content imaging. Methods Mol Biol 2015;1219:35–42.
35. Craveiro V, Yang-Hartwich Y, Holmberg JC, Sumi NJ, Pizzonia J, Griffin B, et al. Phenotypic modifications in ovarian cancer stem cells following Paclitaxel treatment. Cancer Med 2013;2:751–62.
36. Pizzonia J, Holmberg J, Orton S, Alvero A, Viteri O, McLaughlin W, et al. Multimodality animal rotation imaging system (Mars) for *in vivo* detection of intraperitoneal tumors. Am J Reprod Immunol 2012; 67:84–90.
37. Sumi NJ, Lima E, Pizzonia J, Orton SP, Craveiro V, Joo W, et al. Murine model for non-invasive imaging to detect and monitor ovarian cancer recurrence. J Vis Exp 2014:e51815.
38. Casagrande F, Cocco E, Bellone S, Richter CE, Bellone M, Todeschini P, et al. Eradication of chemotherapy-resistant CD44+ human ovarian cancer stem cells in mice by intraperitoneal administration of *Clostridium perfringens* enterotoxin. Cancer 2011;117:5519–28.

39. Liu M, Mor G, Cheng H, Xiang X, Hui P, Rutherford T, et al. High frequency of putative ovarian cancer stem cells with CD44/CK19 coexpression is associated with decreased progression-free intervals in patients with recurrent epithelial ovarian cancer. Reprod Sci 2013;20:605–15.
40. Steffensen KD, Alvero AB, Yang Y, Waldstrom M, Hui P, Holmberg JC, et al. Prevalence of epithelial ovarian cancer stem cells correlates with recurrence in early-stage ovarian cancer. J Oncol 2011;2011:620523.
41. Tiwari N, Meyer-Schaller N, Arnold P, Antoniadis H, Pachkov M, van Nimwegen E, et al. Klf4 Is a Transcriptional Regulator of Genes Critical for EMT, Including Jnk1 (Mapk8). PLoS One 2013;8:e57329.
42. Dhanasekaran DN, Reddy EP. JNK signaling in apoptosis. Oncogene 2008;27:6245–51.
43. Bubici C, Papa S. JNK signalling in cancer: in need of new, smarter therapeutic targets. Br J Pharmacol 2014;171:24–37.
44. Bennett BL, Sasaki DT, Murray BW, O'Leary EC, Sakata ST, Xu W, et al. SP600125, an anthrapyrazolone inhibitor of Jun N-terminal kinase. Proc Natl Acad Sci U S A 2001;98:13681–6.
45. Agarwal R, Kaye SB. Ovarian cancer: strategies for overcoming resistance to chemotherapy. Nat Rev Cancer 2003;3:502–16.
46. Craveiro V, Yang-Hartwich Y, Holmberg JC, Sumi NJ, Pizzonia J, Griffin B, et al. Phenotypic modifications in ovarian cancer stem cells following Paclitaxel treatment. Cancer Med 2013;2:751–62.
47. Bapat SA.Human ovarian cancer stem cells. Reproduction 2010; 140:33–41.
48. Al Mutairi NJ, Le T. Does modality of adjuvant chemotherapy after interval surgical debulking matter in epithelial ovarian cancer?: An exploratory analysis. Int J Gynecol Cancer 2014;24:461–7.
49. Singer G, Oldt R, 3rd Cohen Y, Wang BG, Sidransky D, Kurman RJ, et al. Mutations in BRAF and KRAS characterize the development of low-grade ovarian serous carcinoma. J Natl Cancer Inst 2003;95: 484–6.
50. Meng Q, Xia Y. c-Jun, at the crossroad of the signaling network. Protein Cell 2011;2:889–98.
51. Bossy-Wetzel E, Bakiri L, Yaniv M. Induction of apoptosis by the transcription factor c-Jun. EMBO J 1997;16:1695–709.
52. Musti AM, Treier M, Bohmann D. Reduced ubiquitin-dependent degradation of c-Jun after phosphorylation by MAP kinases. Science 1997;275: 400–2.